Medical Research Archives

ESMED
European Society of Medicine

OPEN ACCESS

Published: June 30, 2022

Citation Causa-Andrieu P, Gutierrez-Vallecillo J, et al., 2022. Ovarian Teratomas: A Spectrum of Disease. An approximation for radiologists in training, Medical Research Archives, [online] 10(6). https://doi.org/10.18103/mra.v10i6.2800

DOI
https://doi.org/10.18103/mra.v10i6.2800

ISSN: 2375-1924

REVIEW ARTICLE

Ovarian Teratomas: A Spectrum of Disease. An approximation for radiologists in training.

Pamela Causa-Andrieu MD* [1], Maria J Gutierrez-Vallecillo MD [2], Maria E Urga MD[3], Hyesung Kim MD [4], Maria N Napoli MD [2], Alejandra Wernicke MD[3], Carolina RB Chacon MD [2,] Refky Nicola M.Sc.Do [5]

[1.] Radiology Department. Memorial Sloan Kettering Cancer Center, New York, NY, United States.
[2.] Radiology Service. Hospital Italiano de Buenos Aires, Argentina.
[3.] Anatomy Pathology Department. Hospital Italiano de Buenos Aires, Argentina.
[4.] Postgraduate School. Seoul, South Korea National University College of Medicine
[5.] Roswell Park Comprehensive Cancer Center, Buffalo, NY, United States.

* causapamela@gmail.com

ABSTRACT:
Ovarian teratomas are the ovary's most frequent germ cell tumors and can be either mature or immature. Ovarian teratomas can also have a monodermal form; struma ovarii is the most common type and are usually multilocular cystic lesions with variable locules. Another less common types of monodermal lesion are ovarian carcinoids. Mature cystic teratomas are composed of predominantly fat, while immature teratomas have a larger solid component with only small foci of fat. This review article discusses the various types of ovarian teratomas with their respective imaging findings, gross pathological, histopathological, complications, and clinical management.

Keywords: germ cell tumor; ovarian teratoma; dermoid cyst, teratoma, immature; struma ovarii; carcinoma

Introduction

Germ cells are the second most common tumor, following epithelial tumors in women after the age of 20. Most of them are mature cystic teratoma, also known as a dermoid cyst [1-3]. Ovarian teratomas account for approximately 20% of all ovarian neoplasms in adults and 50% of pediatric ovarian tumors [3,4].

The radiological evaluation has a paramount role in diagnosing the different types of ovarian teratomas to guide the treatment planning and follow-up. The imaging modality of choice for the diagnosis and surveillance is ultrasound (US). Computed tomography (CT) is helpful in the evaluation of the presence of fat or calcification. Magnetic Resonance Imaging (MRI) is essential for analyzing malignant potential and differential diagnosis, including identifying nodularity, septations, and enhancement by using chemical shift, fat-suppression techniques, diffusion-weighted/ apparent diffusion coefficient, and contrast enhancement. Before fertility-sparing surgery, MRI is critical for preoperative planning to evaluate the normal ovarian tissue. Also, MRI is essential in the characterization of pediatric ovarian masses because it avoids any ionizing radiation[2,5-8].

This review aims to discuss the types of ovarian teratomas and their complications to help the radiologist make an accurate diagnosis and help the referring physician in the treatment planning. Therefore, this review article thoroughly discusses the imaging findings of the various subtypes of teratomas and their complications and succinctly the pathology and clinical management.

Mature cystic teratoma or dermoid cyst

Mature cystic teratoma or dermoid cysts (MCT) constitute 95% of the benign germ cell tumors [9] and 20% of all ovarian tumors [10]. They usually arise in children and women within a mean age of 30 [3,11,12]. They are an incidental diagnosis in 60% of cases [1].

On *gross pathology (Figure 1)*, they are usually cystic lesions of variable size, up to 10% in 80% of cases [8]. The cystic lesion is most commonly unilocular (88%) but can also be multilocular [10]. The most specific macroscopic finding is the presence of fat [3]. Another important finding is the Rokitansky nodule, which is primarily solid and can infrequently be cystic, either single or multiple, which may have tissues from the three dermal layers [8]. They are usually unilateral and on the right side in 90% of cases [12,13].

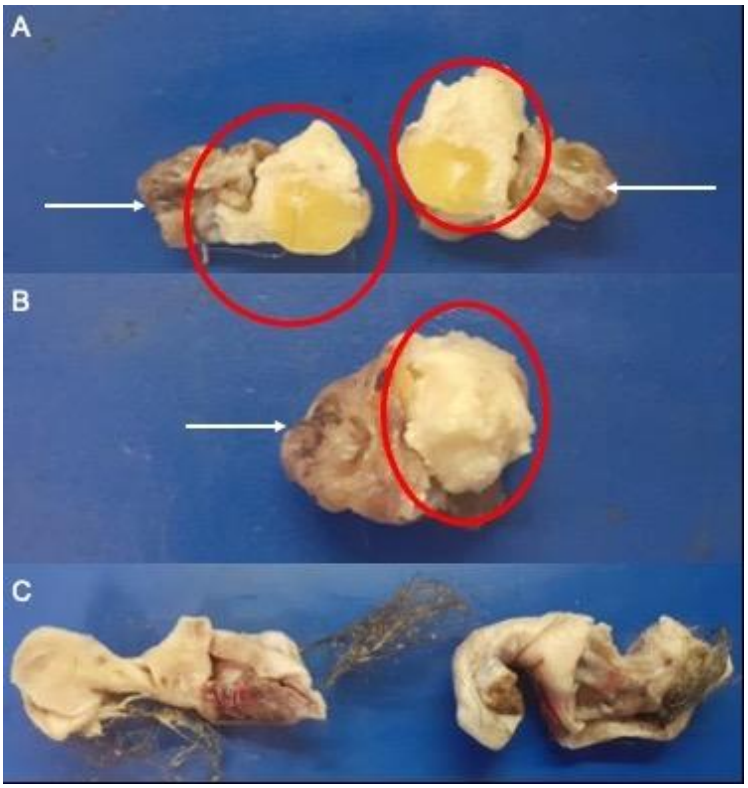

Figure 1. Different appearances of MCT on gross pathology (A-B) Cystic mass (arrow) with pilosebaceous content (circle) and (B) to show the variability of the pilosebaceous content.

In US, MCT can be either unilocular or multilocular cystic lesions. The hyperechogenic regions correspond to fat content, with variable posterior acoustic shadowing. Such hyperechoic areas appear as diffuse homogenous content, mesh-like bands, or scattered particles. In the presence of either fat or fluid, fluid-fluid levels, fluid-fat levels, or floating nodules can occur. Although slightly difficult to distinguish on US, posterior acoustic shadowing is seen with an echogenic Rokistansky nodule which does not demonstrate any Doppler signal [10]. To avoid underdiagnosis of MCT is essential to distinguish the adnexa from the surrounding fat or a fat-containing adnexal lesion on US by using harmonic and grayscale imaging, which helps increase the contrast between the different fat tissues, and Doppler US, which supports delineating the cystic lesion wall [10]. *Figure 2* shows other appearances of MCT in US.

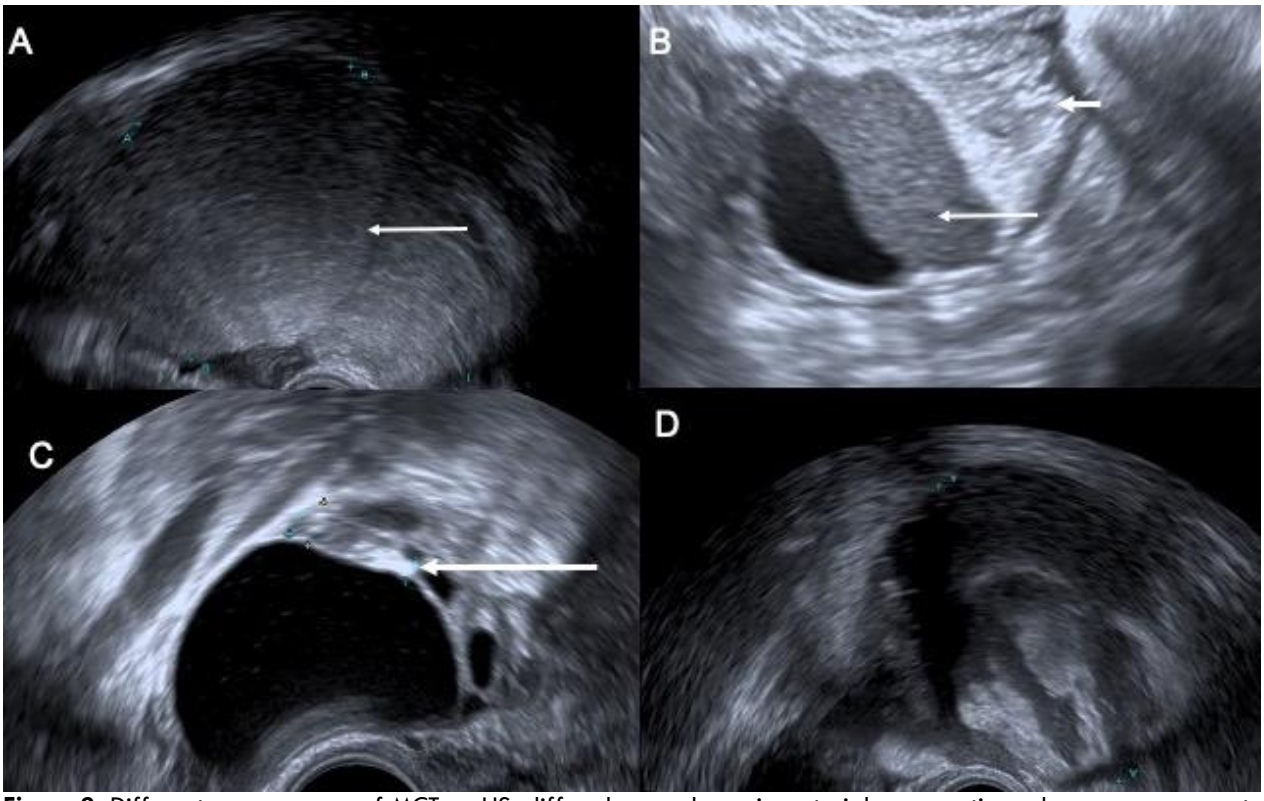

Figure 2. Different appearances of MCT on US: diffuse hyperechogenic material representing sebaceous component (A), fluid-fat levels (B), a focal echogenic area corresponding to fat tissue (C), and floating nodules of variable echogenicity (D).

CT confirms the diagnosis of MCT in more than 90% of cases with the presence of fat (93%), Rokitansky nodule (81%), ectoderm such as teeth or hair (65%), calcifications (56%), and floating mass of hair in the fluid-fat interface [3,8 6] as seen on *Figure 3*.

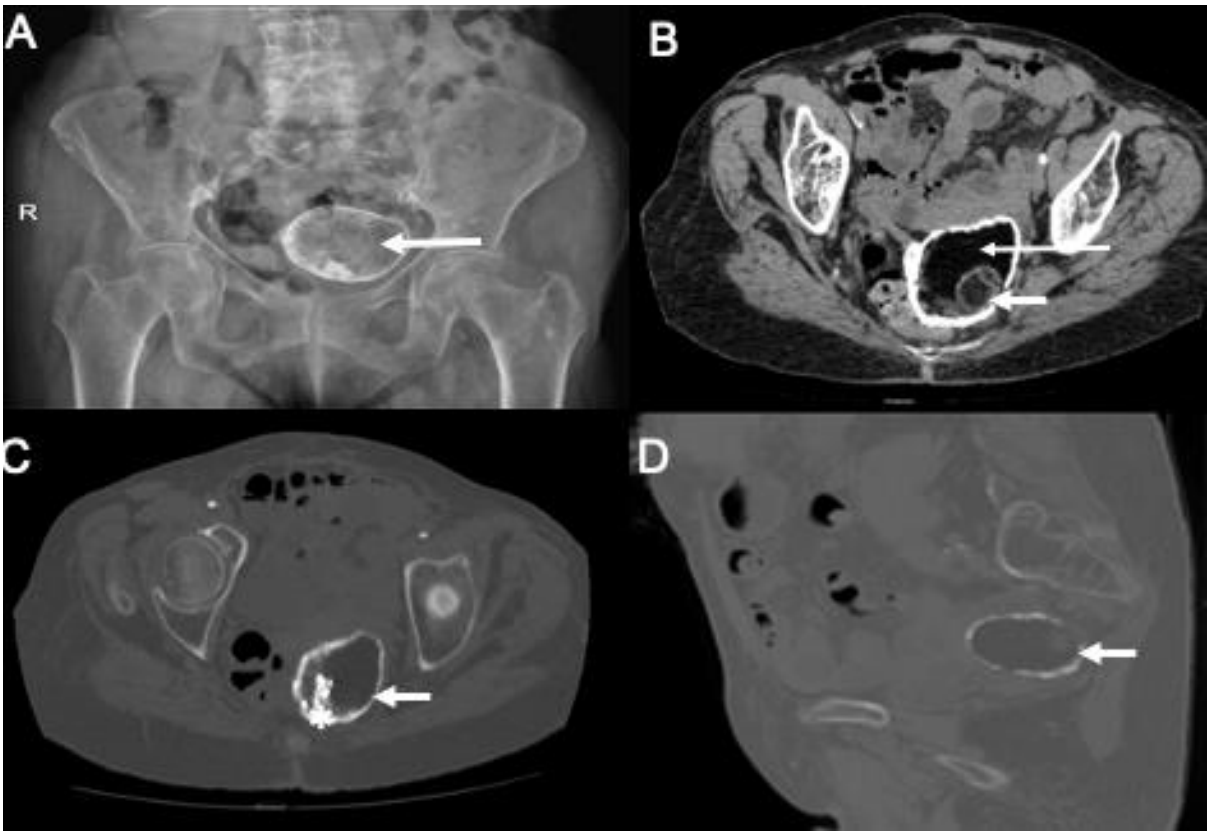

Figure 3. MCT on a pelvic radiograph (A) was performed due to trauma. Further evaluation with CT in soft-tissue (B) and Bone (C, D) windows shows the calcification of the wall (short arrow), the fat component (long arrow), and a tooth (asterisk).

On *MRI*, MCT has a cystic component with fat and a Rokitanky nodule and is rarely within the wall [10]. Fat is hyperintense on the T1-weighted sequence, drops out on the fat-suppressed T1 sequence, and may restrict diffusion-weighted images(*Figure 4*). This should not be confused for a more hypercellular solid tissue mass, such as an immature teratoma. In such a case, a correlation with T1 and T2 weighted sequences is recommended because they can have signal characteristics similar to the subcutaneous or visceral fat [10]. The Rokitansky nodule is an internal nodular or linear structure of variable size and content, with fat, skin, appendages, and calcifications [8]. The Rokitansky nodule has variable enhancement on dynamic contrast enhancement analysis and should not be used to evaluate cellularity. *Figures 3-8* show different appearances of MCT on MRI, and *Figure 9 shows* the correlation between US, CT, and MRI.

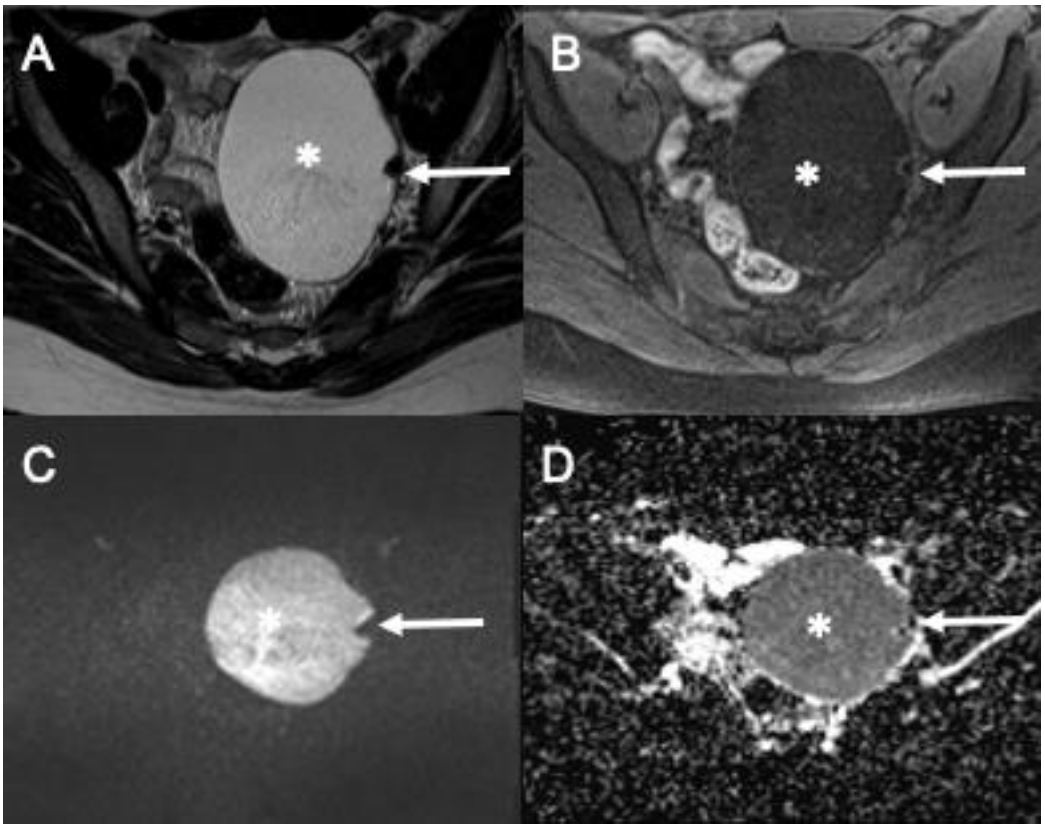

Figure 4. MRI of MCT with mild restricted diffusion. MRI shows a unilocular cystic lesion with a hyperintense signal on T2-weighted image (A) but a loss of signal on T1-fat suppression (B) corresponding to fat tissue (asterisks). The lesion demonstrates mild restricted diffusion (C: diffusion, B value: 1000 sec/mm3; D: attenuation diffusion coefficient) without implying cellularity. A nodule is noted, which is hypointense both on T2 (A) and T1-fat suppression (B), and does not have restricted diffusion (C, D) and corresponds to the Rokitansky nodule (long arrow).

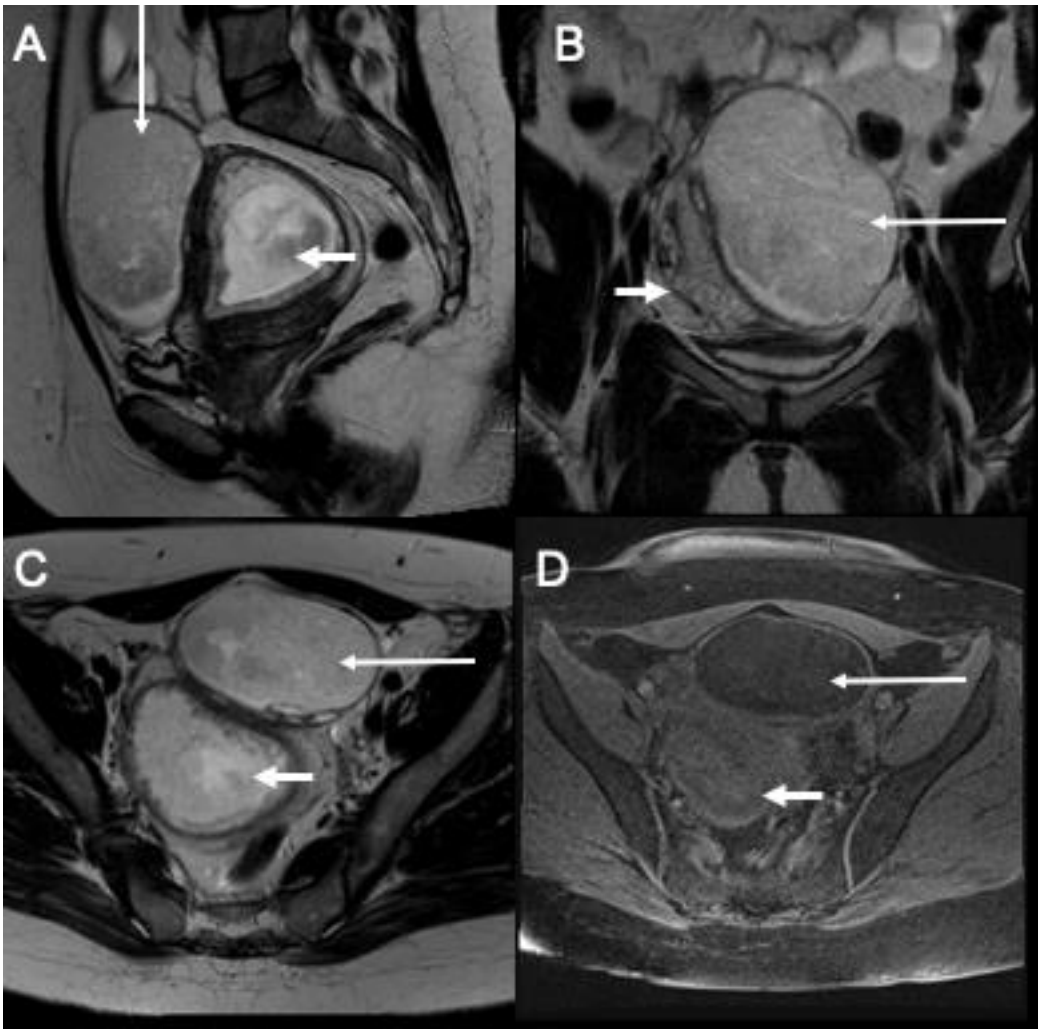

Figure 5. MCT in a pregnant woman evaluated with MRI. Thin-walled cystic lesion with predominantly adipose content (long arrow) located in front of the gravid uterus (short arrow). The fat is the slightly heterogeneous signal on T2-weighted images (A, B, C) and shows a signal loss on T1 fat-suppression (D).

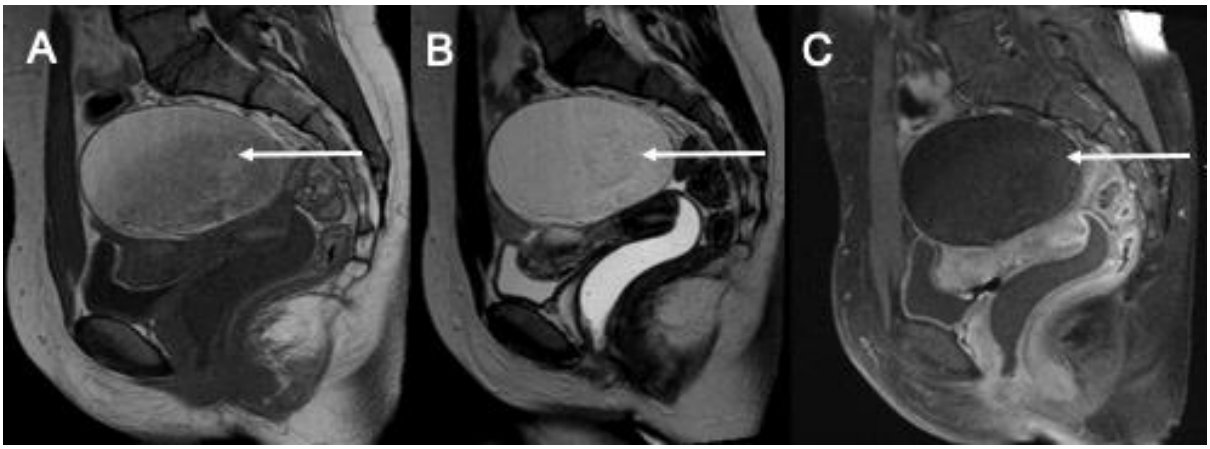

Figure 6. MRI of a unilocular MCT: a unilocular cyst with homogenous high signal on T1-weighted (A) and T2-weighted images (B), with loss of signal on T1-fat suppression (C) corresponding to adipose tissue.

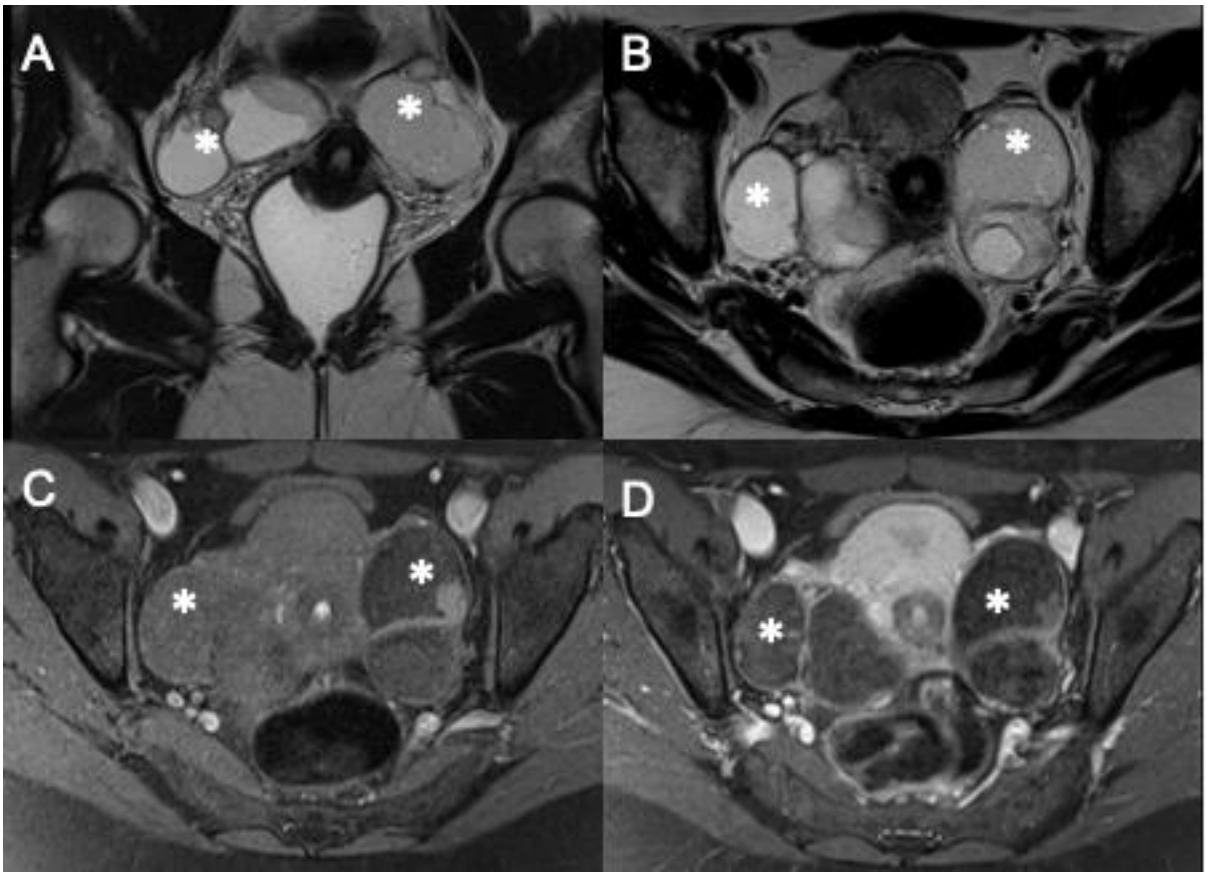

Figure 7. MRI of bilateral MCT: both ovaries show bilobed cystic lesions (asterisks) with component hyperintense on T2-weighted images (A, B) that lose signal on T1-fat suppression weighted imaging (C, D).

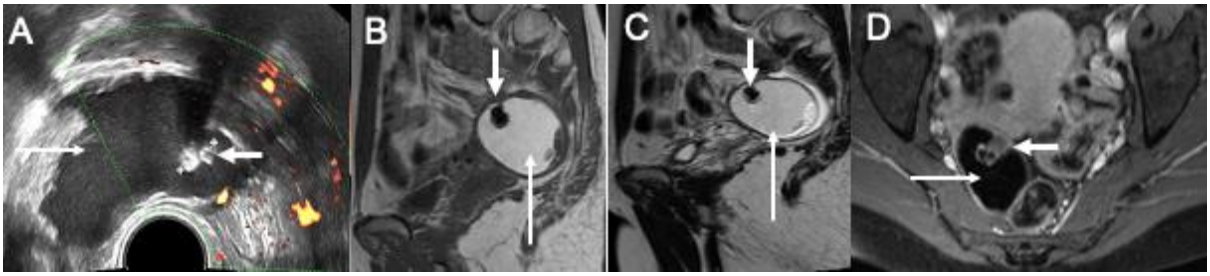

Figure 8: US and MRI of MCT to show a Rokitansky nodule. (short arrows). US (A) shows a unilocular cystic lesion with an echogenic nodule without flow in the Doppler exam. On MR, it is hypointense on T1-weighted (B) and T2-weighted (C), and subtle enhancement contrast (D). The fat tissue component (long arrows) is slightly echogenic on US (A), high signal on T1-weighted (B) and T2-weighted (C), and loss of signal on fat-suppression images (D).

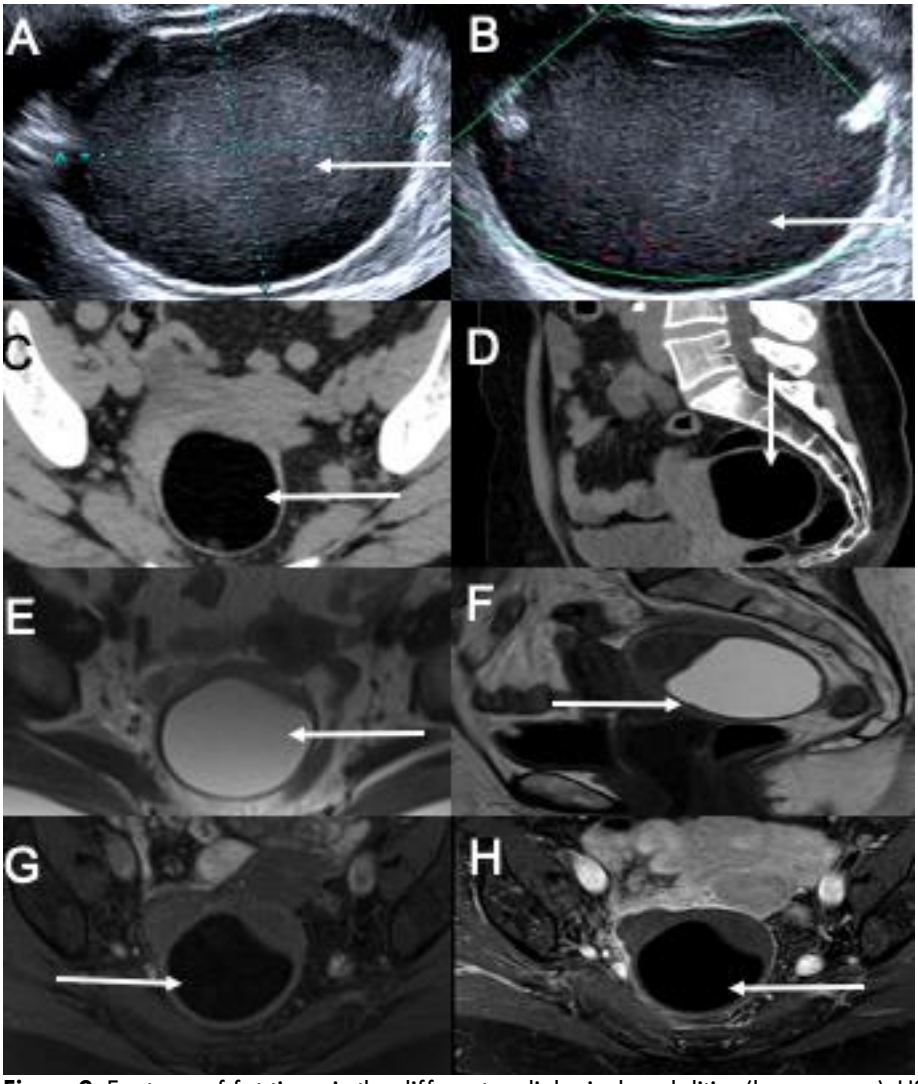

Figure 9. Features of fat tissue in the different radiological modalities (long arrows). US shows a unilocular cystic lesion diffusely echogenic (A) without flow in the Doppler exam (B). On CT (C, D), it has a similar density to the subcutaneous and visceral fat. Moreover, on MR, it is hyperintense on T2-weighted (E) and T1-weighted (F), with loss of signal in T1-fat suppression (G-H).

The *differential diagnosis* of MCT includes functional hemorrhagic cyst, endometrioma, or cyst adenofibroma (Figure 10). A hemorrhagic functional cyst usually has intense and peripheral color Doppler in the US. On MRI, a hemorrhagic cyst has hyperintensity on T1-weighted sequence and intense rim-enhancement on post-contrast images, which resolves with subsequent imaging. To distinguish endometriomas from MCT in the US, variable danders with multiple hyperechoic lines and possible associated fluid-fluid levels due to the sebum component favor the latter [10]. On MRI, endometriomas usually appear as cystic lesions with high signal intensity on T1-weighted images and intermediate to low signal on T2-weighted images, known as "T2 shading" due to the presence of bleeding in different stages. They can also show mild restricted diffusion due to their high protein content, which should not be confused with a sign of cellularity. Commonly, the wall enhances less than a normal follicle or functional cyst. They are hyperintense due to bleeding in fat-saturated T1-weighted images [14]. Ovarian cystoadenofibromas are benign tumors with epithelial and fibrous stromal components. The fibrous stromal component has low signal intensity on T2-weighted images, lacks restricted diffusion, and has subtle and progressive enhancement on dynamic post-contrast sequences [15].

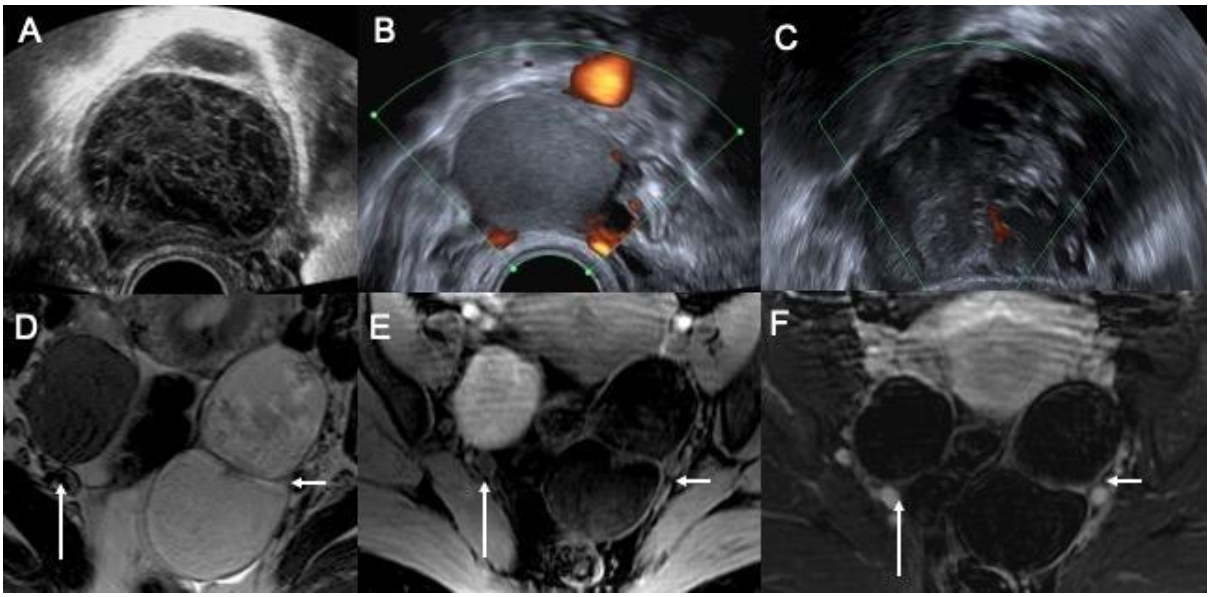

Figure 10. Differential diagnosis. In US: A) Functional hemorrhagic cyst; B) Endometrioma; C) cystadenofibroma. Differential diagnosis on MRI (D-F). There are bilateral ovarian cystic lesions. Right ovary (long arrows) has a unilocular cystic mass with T2-shading (D), hyperintensity on T1-fat saturated (E), and subtle wall enhancement after contrast (F) consistent with an endometrioma. Left ovary has a bilobed cystic lesion (short arrows) with a high signal component on T2 (D) that loses signal on T1 FS (E) and also subtle, subtle wall enhancement after contrast (F) consistent with an MCT.

Complications

The most common *complication* is torsion which occurs 3% -16% [3,4]. As the lesion grows bigger than 6-11 cm (7), the likelihood of torsion increases. In US, there is evidence of an enlarged ovary, displacement of the follicles to the periphery, and a twisted vascular pedicle (present in 88% of cases in a study by Lee et al. [16]). On CT/MRI, ipsilateral fallopian tube enlargement and thickening, ipsilateral uterine deviation, and positioning of the adnexal mass in the midline are usually associated with surrounding inflammatory findings such as striation of adjacent mesenteric fat and ascites [3,4,17]. With ovarian necrosis, there is no contrast enhancement or minimal or no arterial or venous flow on US [11,16] [Figure 11]

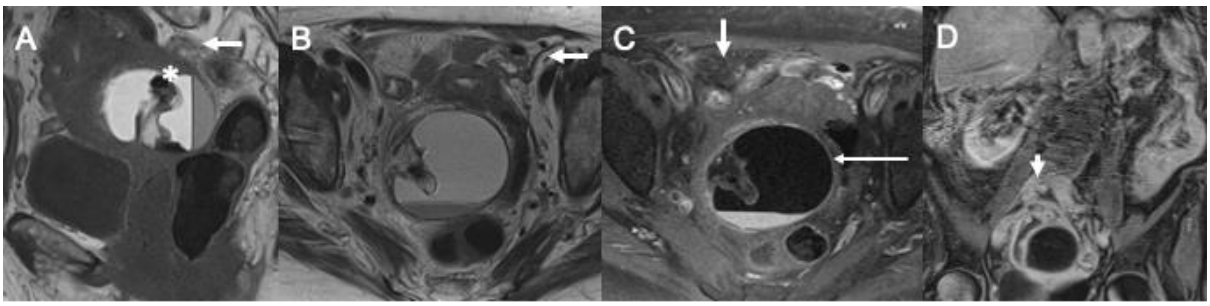

Figure 11. MRI of ovarian torsion due to MCT. MRI (A: T1-weighted; B: T2-weighted; C: axial T1-contrast; D: coronal T1-contrast) shows a cystic lesion consistent with MCT (asterisk) with a lack of enhancement on post-contrast images (long arrow). In addition, there are associated fat stranding (short arrows) and a twisted pedicle (arrowhead).

The uncommon complication (1-4%) of MCT is rupture [3]. Rupture can occur spontaneously or after ovarian torsion [18]. On CT, rupture is evident with the distortion of the mass contour, lack of wall continuity, and free fluid with free fat cells [18]. As a result, rupture causes acute peritonitis. In addition, chronic tumor leakage causes chronic peritonitis [3].

The *malignant transformation* [Figure 12] occurs in 0.17% to 3.5% of MCT and can occur from any dermal layer [1] and more commonly in postmenopausal women. It is often a squamous cell carcinoma in 80% of cases, followed by carcinoid tumor and adenocarcinoma. The transformation occurs within the Rokitansky nodule, which shows transmural growth [3]. On MRI, an ill-defined and

irregular component with possible invasion of adjacent structures suggests the presence of tumor, which has intermediate to high signal on T2 weighted sequence, restricted diffusion, and intense and early enhancement. In addition, the fat component may disappear; thus, the underlying MCT is less conspicuous [1,4,8,9,12,19].

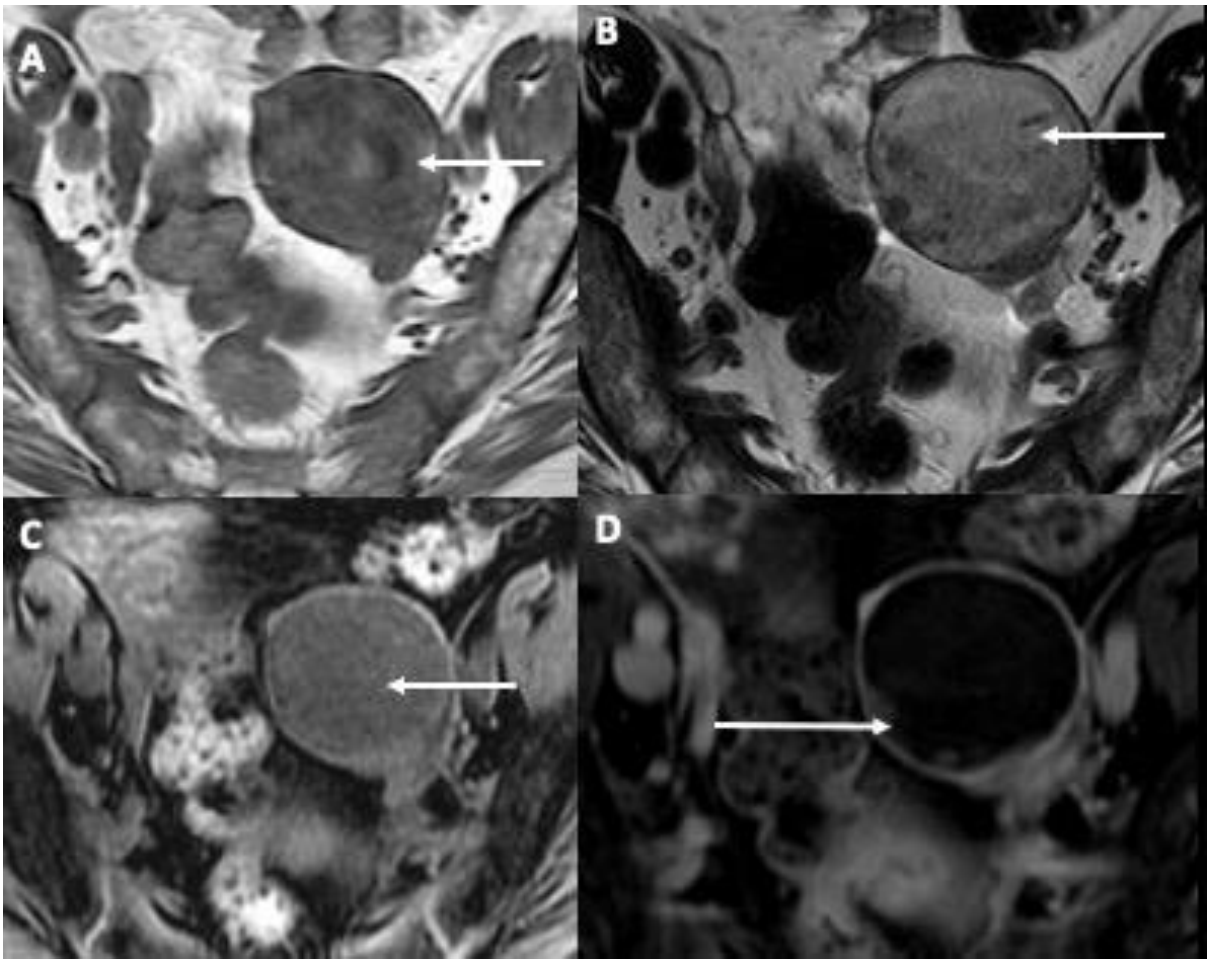

Figure 12: MRI of a squamous cell carcinoma arising from an MCT. MRI shows a left ovarian unilocular cystic lesion with heterogenous component (long arrows) on T1 (A), T2 (B), and T1 without contrast (C) that has loss of signal on T1-fat saturated post-contrast (D) suggestive of fat component. In addition, on T1-fat saturated after contrast (D), enhancing nodular areas on the wall are delineated as suggestive of malignant degeneration (long arrow)

Immature teratoma

Immature teratoma represents 3% of ovarian teratomas, 20% of ovarian germ cell tumors, and 1% of all ovarian malignancies [10]. A MCT and immature teratoma can coexist in the same (26%) or contralateral ovary (10%) [10]. It usually affects women in the first two decades of life [8] and results in an elevated alfa-fetoprotein in most women [10]. Immature teratomas have more malignant potential with a worse prognosis [3,8]. They are usually unilateral in 90% of cases and larger than MCT, with an average diameter of 18 centimeters, and have areas of necrosis and hemorrhage [1].

On gross pathology, immature teratomas are usually larger than MCT and have mostly solid components with small cysts filled with serous or mucinous fluid or fatty sebaceous material. They also have regions of necrosis or hemorrhage. On *histopathology*, immature embryonic tissues have regions that are considered either low or high grades, depending on the tumor grade [1].

US findings are non-specific and variable. It usually resembles an MCT but with an appreciable and varying Rokitansky nodule, without a specific pattern on color Doppler examination [10]. On *CT*, it is a solid mass with irregular borders and variable

regions of calcifications, and tiny areas of fat tissue [10]. On *MRI*, they can appear as either predominantly cystic, predominantly solid, or solid-cystic. There is a characteristic pattern of the solid portion, which is the presence of multiple cysts of variable size with tiny areas of fat tissue [20]. The solid component has intermediate to high-signal on T2-weighed images, restricted diffusion, and perfusion curve type 2 or 3. Also, MRI can show tumoral necrosis and hemorrhage [10] [Figure 13].

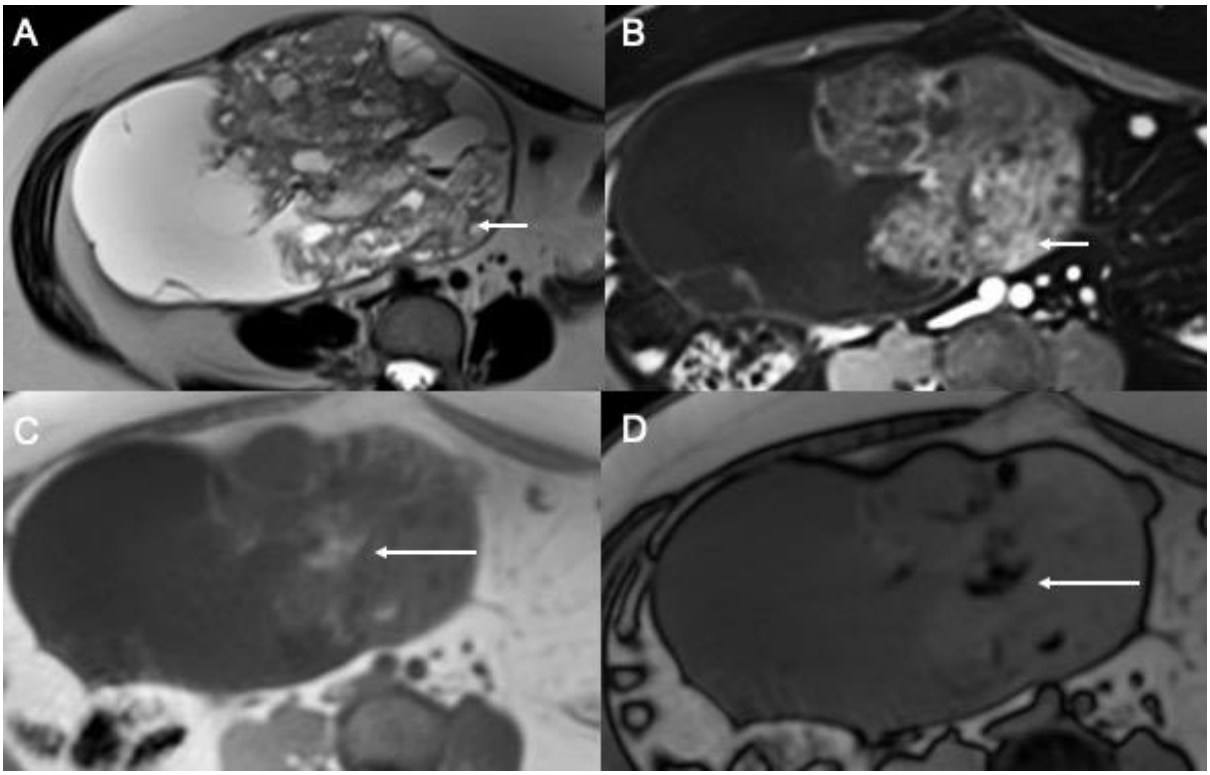

Figure 13: MRI of an immature teratoma: there is a solid and cystic mass in the right ovary, which has small areas of fat component (white arrows) demonstrated by loss-of-signal on the opposed phase (C and D). After contrast administration, the solid areas show intense enhancement (B, short arrows).

Since immature teratoma is more aggressive than MCT, the management will vary depending on patients' desire for fertility, tumor grade, stage, and tumor markers. Therefore, preoperative imaging to assess the extent of disease before resection or adjuvant chemotherapy [7].

Monodermal Teratomas

These are the least common types of teratomas. They contain either ectodermal or endodermal tissue. There are three histological types: struma ovarii, carcinoid tumor, and tumors with neural differentiation [3,8].

***Struma ovarii*.**

Strumma ovarii is the most common monodermal teratoma and is only 3% of ovarian teratomas [1,8]. 95% of them are benign and affect pre-menopausal women. More than 50% of teratoma have thyroid tissue; thus, 5% of patients can present with symptoms of thyrotoxicosis. It may present with ascites and pleural effusion constituting pseudo-Meigs syndrome, which occurs in up to one-third of cases [1,8,19].

In the US and MRI [Figure 14], strumma ovarii is usually a multilocular cystic lesion with locules of different echogenicity or signal intensity, representing the colloidal or gelatinous material without containing fat. Such gelatinous material will have high and low signal intensity on T1- and T2-weighted images. In addition, the internal septations can have variable enhancement [1,4,8].

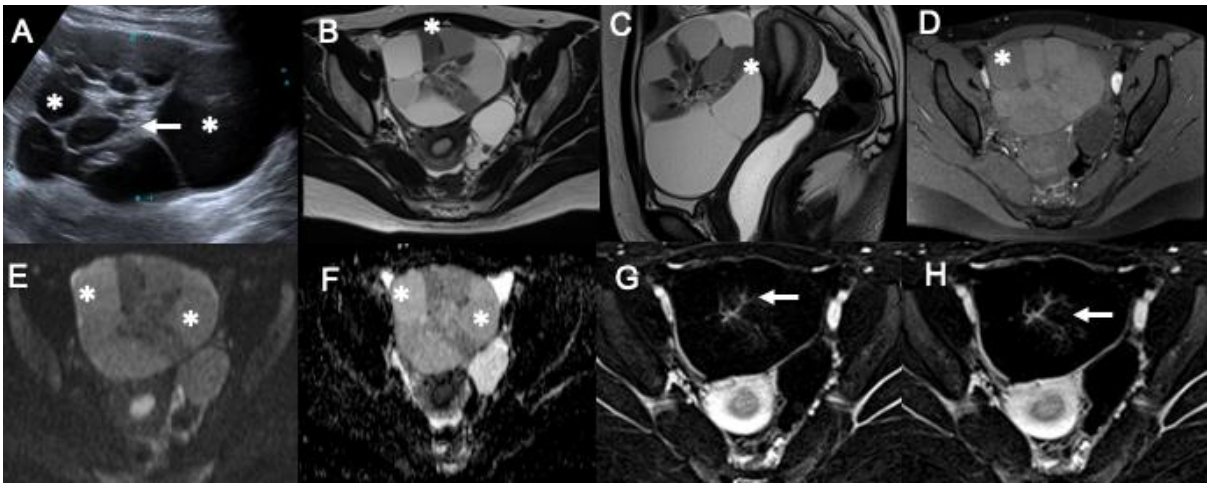

Figure 14: MRI of a strumma ovari. US (A) shows a multilocular cystic lesion with locules of different echogenicity (asterisks) and thickened septations (arrow). On MRI, the locules have variable signal intensity. Still, characteristically there are some with low signal on T2-weighted (B, C) and T1-weighted images (D), as well as mild restricted diffusion (E, F) due to high content on proteins. The septations show mild enhancement on early (G) and delayed (H) enhancement.

Collision Tumors

Collision tumors are composed of different types of teratomas. A collision tumor refers to two histologically different tumors separated by a stroma without histology within the same tumor. While they are rare, the most frequent combination is usually MCT and mucinous neoplasm. This should be considered when an ovarian teratoma has imaging findings that the diagnosis of ovarian teratoma alone cannot explain. A possible association is MCT and struma ovarii [Figure 15] [3,8].

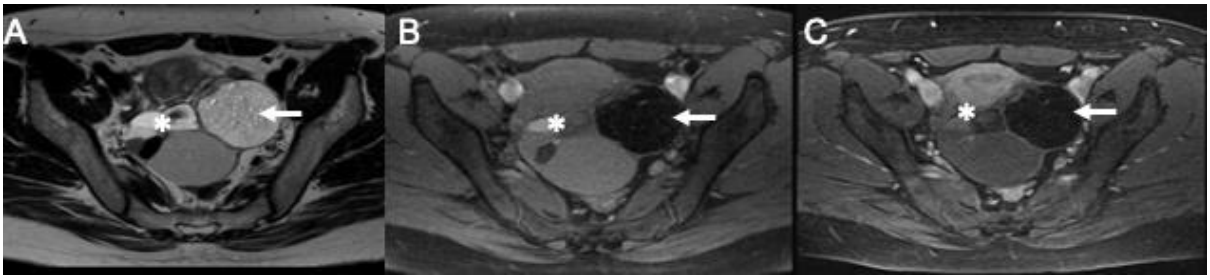

Figure 15: MRI of collision tumor. Collision tumor in the left ovary of a struma ovary (asterisk) and MCT (arrow). A) Axial T2-weighted image. B) Axial T1-weighted image with fat suppression. C) Axial T1 FS G. Multi-locular cyst with multiple loci with different signal intensity (asterisk), corresponding to struma ovarii.

There are usually multicystic lesions on gross pathology representing multiple thyroid follicles of different sizes with a fibromatous or edematous stroma [1].

The *primary differential diagnosis* is a mucinous ovarian tumor, having both overlapping features. In such cases, the visualization of an associated MCT would favor the diagnosis of struma ovary [10].

Carcinoid tumors

It is a rare ovarian tumor (0.3%) that is part of a gastrointestinal carcinoid tumor. It usually occurs in perimenopause or early post-menopause women. It is generally unilateral and can metastasize in a minority of cases. It can arise either as a carcinoid or associated with other tumors such as cystic teratoma, struma ovarii, and mucinous tumors [1,8,10]. On MRI, it is a solid mass with a hypointense T2 signal, restricted diffusion, and intense enhancement [10]. Few papers reported the utility of gallium-68 dotatate in evaluating such tumors due to their somatostatin receptor expression. Such a modality can aid both diagnosis and staging [21].

Management

MCT can be treated conservatively, and if needed, ovarian cystectomy can be performed to achieve a definitive diagnosis and avoid complications [19]. Cystectomy is performed for young women with smaller cystic teratomas to preserve fertility [22]. The

cystectomy can be performed either laparoscopically or via laparotomy, although there is some debate about the size criteria for surgical resection (e.g., more than 10 cm) [17,19]. If there is suspicion of malignancy, the patient should undergo surgical staging and optimal cytoreduction [23]. Radiological evaluation, either with CT or MRI, according to the centers and expertise, is helpful to stage the patient pre-operatively and be a roadmap for the surgeon. [24,25]. In cases of malignant struma ovarii, adjuvant radioactive Iodine (I-131) therapy can be administered due to the thyroid tissue component of such tumors [26].

Conclusion

The characteristic finding of MCT is the presence of fat, which has distinctive features in US, CT, or MRI. The visualization of a new ill-defined soft tissue within an MCT should raise the suspicion of malignancy. Immature teratoma is larger masses with a primarily solid component but can have small cysts and regions of fat. Finally, finding a multilocular cystic tumor with locules of different echogenicity and signal intensity suggests the diagnosis of struma ovari.

Funding: This research was funded in part through the NIH/NCI Cancer Center Support Grant P30 CA008748.

Conflicts of Interest: None.

Ethical standards: this study was approved by the IRB.

Informed consent: it was waived for this retrospective investigation by the IRB as this study was of minimal risk, and data were deidentified.

Consent for publication: all authors expressed explicit consent for the publication of this manuscript.

References

1. Euscher ED. Germ Cell Tumors of the Female Genital Tract. *Surg Pathol Clin*. 2019;12(2):621-649.
2. Mohaghegh P, Rockall AG. Imaging strategy for early ovarian cancer: characterization of adnexal masses with conventional and advanced imaging techniques. *Radiographics*. 2012;32(6):1751-1773.
3. Srisajjakul S, Prapaisilp P, Bangchokdee S. Imaging features of unusual lesions and complications associated with ovarian mature cystic teratoma. *Clin Imaging*. 2019;57:115-123.
4. Park SB, Kim JK, Kim KR, Cho KS. Imaging findings of complications and unusual manifestations of ovarian teratomas. *Radiographics*. 2008;28(4):969-983.
5. Bakir B, Bakan S, Tunaci M, et al. Diffusion-weighted imaging of solid or predominantly solid gynaecological adnexial masses: is it useful in the differential diagnosis? *Br J Radiol*. 2011;84(1003):600-611.
6. Buy JN, Ghossain MA, Moss AA, et al. Cystic teratoma of the ovary: CT detection. *Radiology*. 1989;171(3):697-701.
7. Iavazzo C, Vorgias G, Iavazzo PE, Gkegkes ID. Fertility sparing approach as the standard of care in young patients with immature teratomas. *J Turk Ger Gynecol Assoc*. 2017;18(1):43-47.
8. Outwater EK, Siegelman ES, Hunt JL. Ovarian teratomas: tumor types and imaging characteristics. *Radiographics*. 2001;21(2):475-490.
9. Shaaban AM, Rezvani M, Elsayes KM, et al. Ovarian malignant germ cell tumors: cellular classification and clinical and imaging features. *Radiographics*. 2014;34(3):777-801.
10. Bazot M. *Imagerie de la femme: gynecologie*. Vol 12017.
11. Chen VW, Ruiz B, Killeen JL, et al. Pathology and classification of ovarian tumors. *Cancer*. 2003;97(10 Suppl):2631-2642.
12. Sahin H, Abdullazade S, Sanci M. Mature cystic teratoma of the ovary: a cutting edge overview on imaging features. *Insights Imaging*. 2017;8(2):227-241.
13. Wang W-C, Lai Y-C. Evidence of metachronous development of ovarian teratomas: a case report of bilateral mature cystic teratomas of the ovaries and systematic literature review. *J Ovarian Res*. 2017;10(1):17-17.
14. Foti PV, Attinà G, Spadola S, et al. MR imaging of ovarian masses: classification and differential diagnosis. *Insights into imaging*. 2016;7(1):21-41.
15. Wasnik A, Elsayes K. Ovarian cystadenofibroma: A masquerader of malignancy. *Indian J Radiol Imaging*. 2010;20(4):297-299.
16. Lee EJ, Kwon HC, Joo HJ, Suh JH, Fleischer AC. Diagnosis of ovarian torsion with color Doppler sonography: depiction of twisted vascular pedicle. *J Ultrasound Med*. 1998;17(2):83-89.
17. Chang CK, Teng SW, Leu FJ. Laparoscopy versus laparotomy for cystic ovarian teratomas. *Int J Gynaecol Obstet*. 2005;88(1):69-70.
18. Magudia K, Menias CO, Bhalla S, et al. Unusual Imaging Findings Associated with Germ Cell Tumors. *Radiographics*. 2019;39(4):1019-1035.
19. Sinha A, Ewies AA. Ovarian Mature Cystic Teratoma: Challenges of Surgical Management. *Obstet Gynecol Int*. 2016;2016:2390178.
20. Yamaoka T, Togashi K, Koyama T, et al. Immature teratoma of the ovary: correlation of MR imaging and pathologic findings. *Eur Radiol*. 2003;13(2):313-319.
21. Gupta N, Dougall P, Mahawar S. Primary ovarian carcinoid and dotanoc positron emission tomography-computed tomography scan. *World J Nucl Med*. 2019;18(1):69-70.
22. (RCOG) RCoOaG. Management of Adnexal Masses in Premenopausal Women. . *UK: Royal College of Obstetricians and Gynaecologists (RCOG); 2011*. 2011.
23. Brown J, Friedlander M, Backes FJ, et al. Gynecologic Cancer Intergroup (GCIG) consensus review for ovarian germ cell tumors. *Int J Gynecol Cancer*. 2014;24(9 Suppl 3):S48-54.
24. Ulaner G. *Fundamentals of Oncologic PET/CT. 1st Edition.* . Elselveier,Inc. ; 2019.
25. Javadi S, Ganeshan DM, Qayyum A, Iyer RB, Bhosale P. Ovarian Cancer, the Revised FIGO Staging System, and the Role of

Imaging. *AJR Am J Roentgenol*. 2016;206(6):1351-1360.

26. DeSimone CP, Lele SM, Modesitt SC. Malignant struma ovarii: a case report and analysis of cases reported in the literature with focus on survival and I131 therapy. *Gynecol Oncol*. 2003;89(3):543-548.